PNAS RESEARCH ARTICLE | BIOPHYSICS AND COMPUTATIONAL BIOLOGY

Genetic switching by the Lac repressor is based on two-state Monod–Wyman–Changeux allostery

Julija Romanuka[a,1], Gert E. Folkers[a], Manuel Gnida[a,2], Lidija Kovačič[a,3], Hans Wienk[a,4], Robert Kaptein[a], and Rolf Boelens[a,5]

Edited by William Eaton, National Institute of Diabetes and Digestive and Kidney Diseases, Bethesda, MD; received July 7, 2023; accepted October 26, 2023

High-resolution NMR spectroscopy enabled us to characterize allosteric transitions between various functional states of the dimeric *Escherichia coli* Lac repressor. In the absence of ligands, the dimer exists in a dynamic equilibrium between DNA-bound and inducer-bound conformations. Binding of either effector shifts this equilibrium toward either bound state. Analysis of the ternary complex between repressor, operator DNA, and inducer shows how adding the inducer results in allosteric changes that disrupt the interdomain contacts between the inducer binding and DNA binding domains and how this in turn leads to destabilization of the hinge helices and release of the Lac repressor from the operator. Based on our data, the allosteric mechanism of the induction process is in full agreement with the well-known Monod–Wyman–Changeux model.

gene regulation | repressor | allostery | NMR | structural biology

Significance

Gene regulation is an essential step in the expression of DNA. A well-known gene regulator is Lac repressor which regulates the expression of bacterial lactose genes. Thus far, structural understanding of its mode of action is still largely lacking. We analyzed Lac repressor in distinct states related to gene activation and show that it exists in a dynamic equilibrium between two conformations. In one conformation, the Lac repressor forms a tight complex with DNA. In the other, it binds an inducer, causing destabilization of the helices connecting its core and DNA-binding domains, and thereby weakening DNA binding. Our observations favor a mechanism of activation via the Monod–Wyman–Changeux model as it relies on actively shifting defined structural states upon ligand binding.

Cellular signaling and metabolic response are often under control of allosteric regulation, in which a ligand binding event on one site causes effects on a different location in a protein to influence function and/or a secondary ligand binding event. Two classical models are frequently used to explain the mode-of-action of allosteric proteins: the Monod–Wyman–Changeux (MWC) model (1) and the Koshland–Nemethy–Filmer (KNF) model (2). These two models are considered specific examples of generalized models (3), such as the Eigen model (4) or the ensemble allosteric model (EAM) (5). The MWC model or concerted model (nicely summarized in ref. 6) postulates that in the absence of ligands, the protein is in equilibrium between two reversibly accessible states called for historical reasons T (tense) and R (relaxed). Adding an allosteric effector shifts the equilibrium toward the conformation to which it binds with the higher affinity. The protomers of an oligomeric allosteric molecule undergo this transition in a concerted manner. In contrast, the KNF or sequential model supposes that the conformational and affinity effects occur sequentially as a consequence of binding each ligand in the oligomer. In the KNF model, a specific conformation is induced only upon ligand binding via an induced-fit mechanism rather than selection from a pre-existing equilibrium between R and T states as in the MWC model. In a third allosteric model (here called the dynamic model), it is assumed that the effector does not change the conformation of the protein but only its dynamics (for reviews see refs. 7 and 8). This model gained popularity for situations where no conformational difference has been observed between the active and inactive states of the protein (9, 10). More recently, Nussinov and Tsai (11) discussed the dynamic model and provided a cautionary note: "not observing conformational differences does not mean that they are not there." We come back to this issue for the Lac repressor below.

An early example of an allosteric regulatory protein is the Lactose (Lac) repressor, which controls the lac operon. Even though the Lac repressor has been studied extensively, experiments to distinguish between the various allosteric models have remained inconclusive (12, 13). In several publications, M. Lewis and his co-workers have addressed the allosteric mechanism of the Lac repressor (14, 15). Although there was no direct experimental evidence for a specific model, their kinetic calculations, assuming the MWC model, obtained good fits for various thermodynamic parameters (16, 17). Even though suggestive, this cannot be considered as proof as long as other models have not been discarded after having them tested in a similar way. In fact, recently Kortemme and co-workers (18) proposed the dynamic model for Lac repressor allostery, which clearly contradicts the former. In the current study, we have used NMR spectroscopy to provide clear experimental evidence that the allosteric mechanism of the Lac repressor best fits the MWC model.

Essentially, Lac repressor regulates the switch between consumption of lactose or other sugars in *Escherichia coli* (reviewed in ref. 19). When lactose is not available as a nutrient, Lac repressor binds to specific operator sequences of the *E. coli* DNA to repress transcription of the genes required for lactose metabolism. To change to lactose consumption, the natural inducer allolactose (20) or—in a laboratory setting—the non-natural inducer isopropyl β-D-thiogalactoside (IPTG) (21) binds to the Lac repressor and the protein

Author contributions: J.R., G.E.F., R.K., and R.B. designed research; J.R., G.E.F., M.G., L.K., and H.W. performed research; J.R., G.E.F., M.G., L.K., H.W., and R.B. analyzed data; and J.R., G.E.F., R.K., and R.B. wrote the paper.

The authors declare no competing interest.

This article is a PNAS Direct Submission.

[1]Present address: Shell Global Solutions International B.V., 1031 HW Amsterdam, The Netherlands.

[2]Present address: SLAC National Accelerator Laboratory, Menlo Park, CA 94025.

[3]Present address: Novartis Pharma AG, CH-4056 Basel, Switzerland.

[4]Present address: Division of Biochemistry, Netherlands Cancer Institute, 1066 CX Amsterdam, The Netherlands.

[5]To whom correspondence may be addressed. Email: r.boelens@uu.nl.

This article contains supporting information online at https://www.pnas.org/lookup/suppl/doi:10.1073/pnas.2311240120/-/DCSupplemental.

Published November 29, 2023.

lowers its affinity for the *lac* operator, which allows subsequent transcription of the structural lac genes.

Several decades of extensive biochemical and structural studies yielded considerable insight into the architecture and various conformations of the tetrameric Lac repressor (reviewed in refs. 14 and 22). The repressor is best described as a dimer of dimers with two DNA binding sites and four inducer binding sites. Each of the four monomers consists of i) an amino-terminal headpiece (HP, residues 1 to 62) which is responsible for the operator recognition, ii) the protein core with the inducer binding site (63 to 333), and iii) the carboxy-terminal tetramerization helix (334 to 360). The amino-terminal part of the headpiece (residues 1 to 49) comprises a canonical helix-turn-helix (HTH) DNA binding motif (23) that is linked to the core by the so-called hinge region (residues 50 to 62). The inducer binding site is located in the cleft between the N- and C-terminal subdomains of each core. The inducible DNA binding unit of the Lac repressor is the dimer which is held together via an extensive intermolecular interface in the core domain.

When the Lac repressor or the isolated dimeric HP binds with its HTH motif to the major groove of operator DNA, the hinge region between the headpiece and the core folds into an alpha helix. The hinge helix protrudes into the minor groove and introduces a kink in the operator as the Leu56 sidechain intercalates between the central C:G base pair step of the operator (24–27). In fact, a large number of protein–DNA interactions are responsible for the tight complex of the Lac repressor with its operator (26–28). Upon binding of the Lac repressor to the operator, also extensive interactions between the HP of one monomer and the core domain of the other monomer are formed that seem to stabilize the DNA-bound conformation and to keep the lac-gene expression dormant (27). For activation, inducer molecules binding to the Lac repressor cores cause a reorientation of the core N-subdomains which alters both the intramolecular interactions between the N- and C-subdomains of the monomer and the interactions between the two N-subdomains in the dimer (24, 29, 30).

For the allostery of the Lac repressor, there are at least four relevant states: i) free, ii) inducer-bound, iii) operator-bound, and iv) ternary complex. For two of them (inducer- and operator-bound), detailed structural information is available from crystallography; the other two have so far resisted detailed structural analysis. Coordinates are available for the free core of the Lac repressor, but without its DNA binding domain, and for the key-regulatory ternary complex, in which the Lac repressor is bound to operator DNA as well as inducer, detailed structural information is fully lacking even though the existence of such ternary complex was established by kinetic experiments (31).

In addition, results from various studies on the free form of the Lac repressor are inconclusive. For instance, optical and chemical modification studies have demonstrated substantial conformational changes that occur in the core region upon IPTG binding (32–35). In contrast, however, the crystal structure of the apo Lac repressor tetramer (lacking its DNA binding region) is very similar to the structure of the protein bound to IPTG (with a backbone rmsd of only 0.4 Å), but different from the DNA-bound state (24). A later crystal structure of the dimeric IPTG-bound repressor also shows no significant conformational differences with the free state (30).

Advances in methodology and new labeling techniques have considerably extended the size limit of NMR spectroscopy over the years (36–38), which now allows analysis of the dimeric Lac repressor (76 kDa) in various allosteric states under identical conditions. In the present study, we provide detailed structural insight into the free state of the Lac repressor and its ternary complex. For this study, a fully functional dimeric Lac repressor mutant containing a K84M mutation but lacking the tetramerization domain was used (39). The K84M mutation provides a thermostable, yet fully functional and inducible, Lac repressor (40) which allowed extended NMR experiments of all four allosteric states. ^{1}H and ^{15}N chemical shift changes between various functional states of the intact Lac repressor dimer (apo, protein–inducer complex, protein–DNA complex, and protein–DNA–inducer complex) could be monitored and could be mapped on available X-ray structures. Our combined results clearly show that spectral properties of the core of the apo Lac repressor can be described by an equilibrium between only two structural states. This strongly favors a conformation-driven allosteric pathway in full support of the MWC model.

Results

Apo Lac Repressor. The NMR spectra of the core domain without DNA-binding domain and that of the intact dimeric Lac repressor show that both proteins are well structured. To monitor the behavior of their backbone amides, ^{15}N TROSY NMR spectra of the isolated core and HP domains were compared with that of the intact Lac repressor (Fig. 1 *A* and *B*). The absence of significant chemical shift differences of the backbone amides for residues Thr5-Ile48 reveals that the structure of the N-terminal HTH domain is unaffected by the presence of the core. In addition, core residues His112-Ser120 (Fig. 1*D*) that are known to contact HP in the presence of DNA (27), are also unaffected. Combined, these findings imply that there are no substantial direct interactions between the N-subdomain of the protein core and the headpiece in the apo form of the Lac repressor dimer.

In isolated Lac headpiece, the hinge region is fully unstructured (41). In contrast, hinge region residues Asn50, Val52, Ala53, Gln54, Gln55, Leu56, and Ala57 show small but distinct chemical shift differences between the intact Lac repressor and the isolated Lac headpiece (Fig. 1*C*). Analysis of the direction of the shifts indicates that possibly a small fraction (~5%) of the unstructured ensemble of the HP hinge region in intact Lac repressor already occurs in helical conformation even without being bound to DNA. Comparing ^{15}N NMR relaxation data of the isolated monomeric headpiece (residues 1 to 56) (41) and the same headpiece as part of the intact Lac repressor dimer supports this picture (*SI Appendix*, *Text* S1 and Fig. S1 and Table S1). Namely, the overall rotational tumbling for the HTH domain connected to the core is much faster than expected for a rigid system (τ_c = 10.9 ns vs. about 79 ns). On the other hand, the tumbling of the HP in the Lac dimer is significantly slower than that of a free monomeric headpiece (τ_c = 10.9 ns vs. 5.7 ns). Therefore, we conclude that the hinge region is partially ordered when the core is attached to the headpiece.

Remarkably, chemical shift differences between the isolated core domain and the intact dimer containing the headpiece are also seen for residues Asp278, Ser279, and Cys281 in the C-subdomain of the dimerization interface. This implies that long-range (over 40 Å) interactions exist between the C-subdomain and the N-terminal end of the N-subdomain where the headpiece is attached, reflecting an internal link between remote parts of the Lac repressor.

Repressor–Operator Complex. To monitor structural changes and conformational rearrangements associated with specific DNA binding, we compared the NMR spectra of the free Lac repressor dimer free and when bound to its 22-base-pair symmetrical operator (SymL). As expected, the largest effects are observed in the HP region (Fig. 2 *A* and *B*). Analysis of the ^{15}N and ^{1}H chemical shifts of the hinge region residues indicates that a hinge

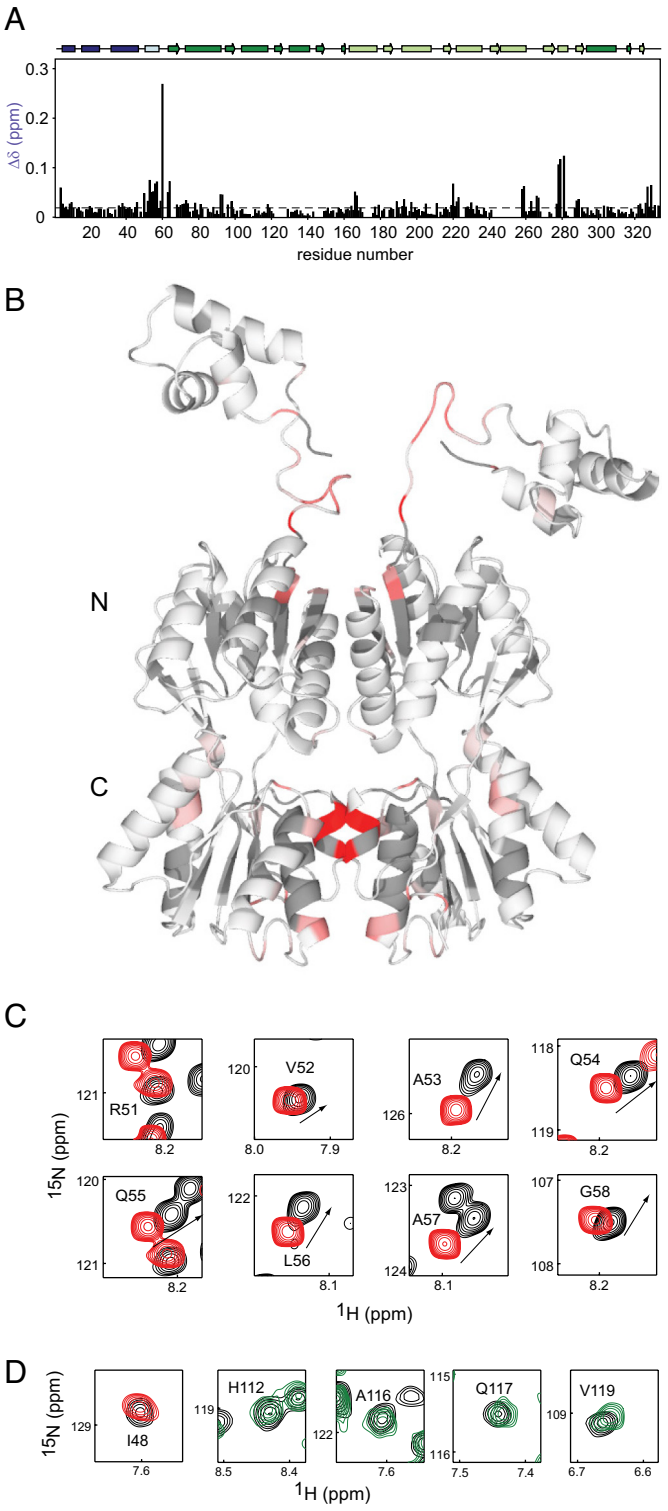

Fig. 1. NMR analysis of the apo form of the Lac repressor dimer. (*A*) Bar diagram of combined ^{1}H and ^{15}N chemical shift changes (Δδ) between the isolated domains [HP (residues 1 to 62) and core domain (residues 60 to 333)] and the intact Lac repressor dimer. α-helical structure elements of the different modules of the Lac repressor are shown at the top of the histogram: The headpiece is shown in dark blue, the hinge region in light blue, the N-subdomain (residues 62 to 161 and 293 to 320) is shown in dark green, and the C-subdomain (residues 162 to 289 and 321 to 329) in light green. (*B*) Δδ values that are larger than average are mapped onto a model of the free Lac repressor dimer, based on combining structures of headpiece (PDB ID 1OSL, residues 1 to 62) and core (PDB ID 1EFA, residues 63 to 331), as a gradient of white-red. Residues that were not assigned either due to overlap or incomplete backbone exchange are shown in a darker shade of gray. (*C* and *D*) Comparison of ^{15}N TROSY spectra of isolated headpiece (red), isolated core (green), and intact Lac repressor dimer (black). Arrows point in the direction of alpha helix formation.

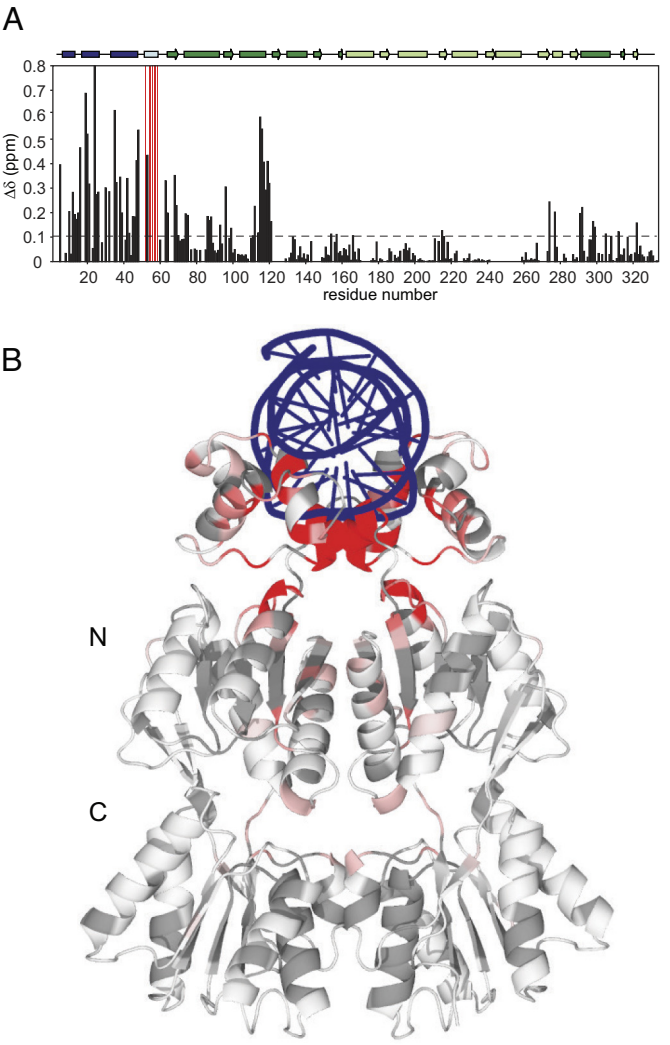

Fig. 2. DNA binding to the Lac repressor dimer. (*A*) The bar diagram shows the differences in chemical shift between backbone resonances of the free protein and the protein bound to the symmetric operator (SymL). The hinge region is shown in red to emphasize formation of the hinge helix. (*B*) Chemical shift changes are mapped onto the crystal structure (PDB ID 1EFA) of the Lac repressor dimer bound to the symmetrical operator and ONPF as a gradient of white-red.

helix is formed similarly as has been shown before for the isolated HP in complex with SymL (26). However, aside from these direct DNA-protein contacts, substantial chemical shift changes were also observed for residues Val111-Gly121 in the core domain that correlate surprisingly well with the interdomain contacts between the Lac dimer core and the headpiece seen in the crystal structure of the repressor–operator complex (27).

A closer look reveals that the spectral changes induced by operator binding to the headpiece propagate all the way through the dimer to residues Ala75 and Asp274 in the inducer binding site using several residues located at the dimerization interface that have been implicated in allosteric signaling before, i.e. Asp88, Ser93, Val96 and Met98 (27). Notably, even residues at the junction of the N- and C-subdomains (residues His74, Glu277, Gln291, and Asp292) near the inducer binding site are affected by operator binding to the remote headpiece, which could reflect a conformational change at the inducer binding site that alters the ligand-binding affinity. Indeed, it has been noted that binding of operator to Lac repressor lowers the affinity for IPTG 20-fold (12).

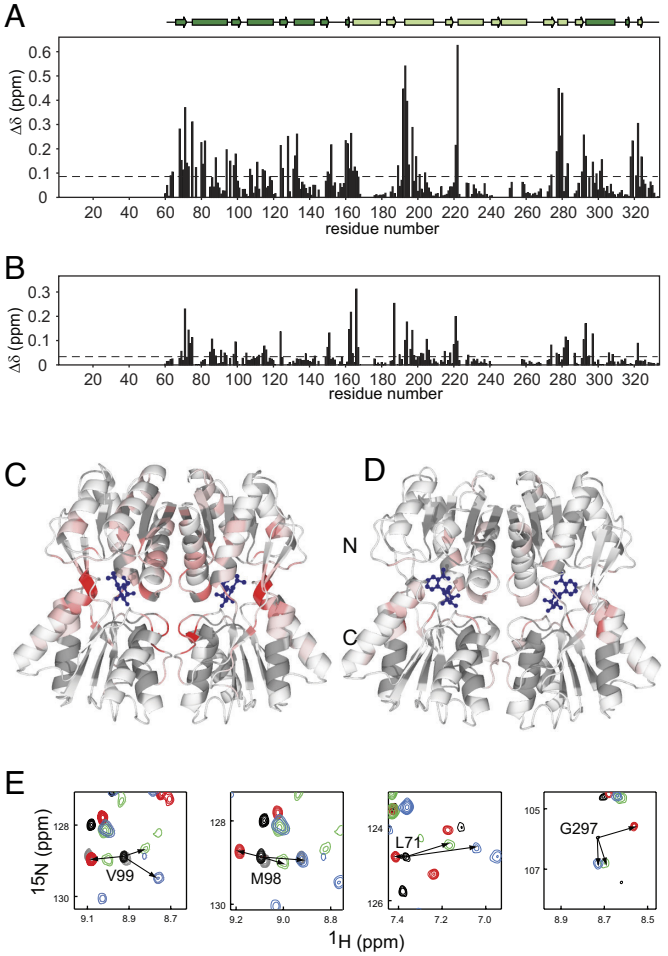

Fig. 3. Lac repressor core dimer binding to inducer IPTG or anti-inducer ONPF. (*A*) The bar diagram shows the differences in chemical shift between backbone resonances of the free and IPTG-bound core domain. (*B*) The bar diagram shows the differences in chemical shift for backbone resonances of the free and ONPF-bound Lac repressor core domain. (*C*) Chemical shift changes shown at (*A*) are mapped onto the crystal structure of the Lac repressor dimer core bound to IPTG (PDB ID 2P9H) as a gradient of white-red. The ligands are shown in blue ball-stick representation. (*D*) Chemical shift changes shown at (*B*) are mapped onto the crystal structure (PDB ID 2PAF) of the Lac repressor dimer bound to ONPF as a gradient of white-red. (*E*) Comparison of ^{15}N TROSY spectra of the free core domain (black), the Lac repressor dimer bound to operator DNA (red), the core domain bound to IPTG (blue), and the core domain bound to ONPF (green).

Inducer and Anti-Inducer Complexes. For NMR titrations with the inducer IPTG and the anti-inducer ONPF, we used the dimer core instead of the intact Lac repressor because of the instability of free Lac repressor (even of the K84M mutant), which would lead to partial degradation during extended measurements. In particular, the hinge helix is prone to cleavage (42). Addition of the inducer molecule IPTG to the apo form of the Lac repressor dimer core domain results in major spectral changes for many residues, including those from the inducer binding site but also at the outer surface of the N-subdomain (Fig. 3 *A* and *C*). Strikingly, changes are also seen for residues Val111-Gly121 that are known to be the anchor points for headpiece in the protein–DNA complex. Many of the observed chemical shift differences, in particular those at the interface between the core N-subdomains, occur in opposite directions to those that we find upon operator binding (Fig. 3*E*), which, as we will explain below is likely due to a shift in conformational equilibrium. Another remaining question for a long time has been whether upon IPTG binding the symmetry of the dimeric core domain would be maintained. To address this, we see that addition of an excess IPTG results in a tight complex with a single set of resonances for the bound conformation, which exchanges only slowly on the NMR chemical shift time scale with the free protein. Furthermore, when the Lac repressor core is only partially saturated with IPTG, the affected residues show only two discrete sets of resonances corresponding to either free or bound conformations of the protein, without evidence of an intermediate form. Together, these results indicate that IPTG binds to the Lac repressor monomers in a highly cooperative fashion, preserving the symmetry of the dimer.

Anti-inducers that inhibit induction, such as orthonitrophenyl-β-D-fucoside (ONPF), compete with IPTG in binding to the Lac monomer inducer binding site (31). NMR titrations of the free Lac repressor core dimer with ONPF show that also anti-inducer binding is in the slow exchange regime, just like binding of IPTG. In contrast to IPTG, however, addition of the anti-inducer ONPF only shows changes in the inducer binding pocket, whereas the signal does not propagate toward the core–HP interface (Fig. 3 *B* and *D*). It is known that the Lac repressor–ONPF complex has increased affinity for DNA relative to the Lac repressor alone (31), which may be due to the Lac repressor–ONPF complex adopting a DNA-bound conformation. However, the direction of the spectral changes upon addition of ONPF to the core Lac dimer does not indicate that ONPF induces such conformation (see below) (Fig. 3*E*). Thus, ONPF appears to compete only with inducer binding but is not itself responsible for stabilizing the repressed state.

Ternary Complex of Lac Repressor, Operator, and Inducer. The formation of a ternary complex by addition of IPTG to the dimeric Lac repressor–SymL complex is associated with a significant structural perturbation as reflected in large chemical shift changes (Fig. 4 *A* and *B*). Not surprisingly, upon titrating, the largest changes occur around the inducer binding site and the detected differences for these residues are quite similar to those found for the operator-devoid Lac core–IPTG complex. However, more importantly, many large spectral changes also occur at sites far away from the inducer binding pocket. Closer inspection shows that IPTG binding causes widespread changes involving residues at the dimerization interface within the N-subdomain (i.e., residues Asp88, Val94, Val96), whereas another strongly affected region is the dimerization interface within the C-subdomains in the dimer (residues Ser221, Ala222, Asp278, and Ser280). In addition, these changes all reflect slow exchange processes, which is in line with the high affinity and slow off-rates that have been reported for the inducer binding to the Lac repressor before (43).

Quite to our surprise, we found no substantial spectral changes in the HTH domain upon IPTG addition to the protein–DNA complex. The absence of these for all residues between Thr5 and Tyr47 indicates that the HTH domain stays bound to operator DNA similarly as in the Lac repressor–DNA complex at NMR concentrations (0.1 mM), which is consistent with the binding constant of the Lac repressor for the operator in the presence of IPTG (K_D ~ 1 μM) (43). In addition to the NMR analyses above, DNA-bending studies revealed that the IPTG-bound repressor bends the bound operator similarly as in the inducer-free protein–DNA complex (Fig. 4*C*), implying that the hinge helix is to a large extent intact. At the same time, however, the amide backbone NMR signals of residues in the hinge region disappeared, likely due to line broadening since there were also no signals found at frequencies corresponding to an unstructured hinge region or elsewhere. Therefore, IPTG-binding at its canonical binding site seems to be accompanied by increased intrinsic dynamics on the millisecond time scale in the hinge-region rather than full helix unfolding. Moreover, several residues that are known to be involved in

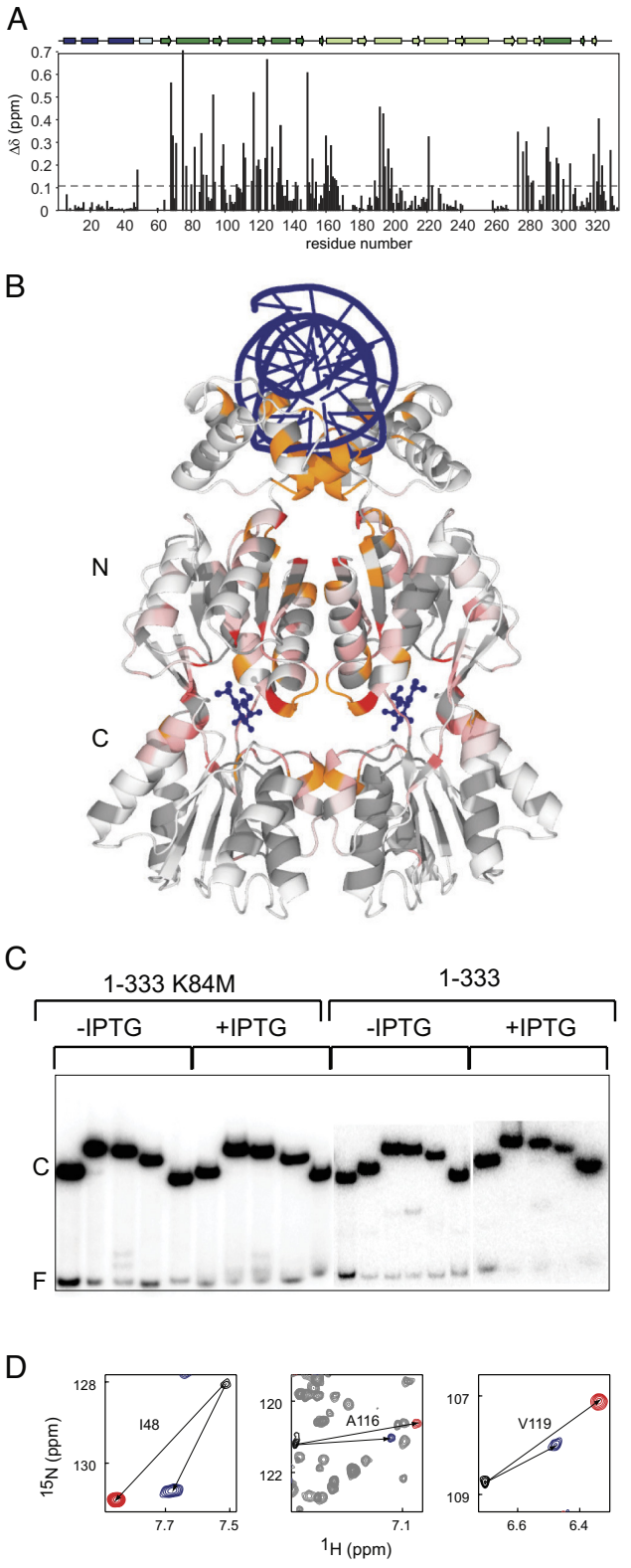

Fig. 4. Ternary complex of the Lac repressor dimer. (*A*) Chemical shift changes between repressor–SymL and repressor–SymL–IPTG complexes. (*B*) Chemical shift changes mapped on a model for the ternary complex, based on the DNA bound Lac dimer (PDB ID 1EFA) with ONPF replaced by IPTG, as a gradient of white-red. Residues that were affected but could not be assigned either due to the line broadening or large signal shift are shown in orange. (*C*) Electrophoretic mobility shift assay using different circularly permuted SymL *lac* operator fragments, showing bending of the operator DNA in the ternary complex. The free probe and the protein–DNA complex are indicated with F and C, respectively. (*D*) Comparison of ^{15}N TROSY spectra of the free Lac repressor dimer (black), Lac repressor dimer bound to DNA (red), and the ternary complex (blue).

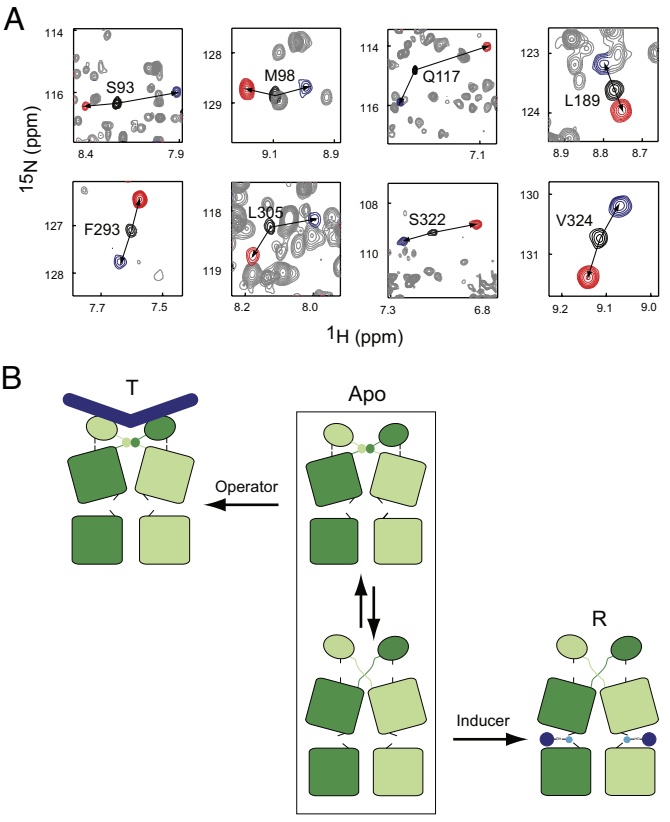

Fig. 5. Comparison of three conformations of the Lac repressor dimer and proposed model for allosteric regulation of the Lac repressor. (*A*) Overlay of ^{15}N TROSY spectra of the free Lac repressor dimer (black), Lac repressor dimer bound to DNA (red), and the ternary complex (blue). (*B*) Free repressor (Apo) in rapid equilibrium between two conformational states, stabilized by either Operator binding (T) or Inducer binding (R).

the core–HP interactions, i.e., Ile48, Val111-Gly121, undergo significant amide signal repositioning upon IPTG addition, clearly showing distinct chemical shift values for all forms of the Lac repressor (Fig. 4*D*) and indicating that the interface between the headpiece and core domain is changed in response to IPTG binding.

Finally, we compared the chemical shifts of the free Lac repressor, Lac repressor bound to its operator and the Lac repressor in the ternary complex for all residues that we could assign. A striking pattern was observed for the amide ^{1}H and ^{15}N chemical shifts of residues in the core N-subdomain that were previously implicated in allostery: It appears in many cases that the resonances for the free Lac repressor lie approximately on a straight line in between those of the repressor–operator complex and the ternary complex and almost in the middle position of that (Fig. 5*A*). *SI Appendix*, Fig. S3 highlights these residues on a model of the ternary complex. Exceptions of this behavior are found near the core–HP interface (Fig. 4*D*) and for residues that directly contact either operator or IPTG. Such a linear pattern is a clear signature of an allosteric apo protein that is in fast conformational equilibrium between two distinct conformations, with the chemical shifts of the apo form representing a population-weighted average of these two. From the data in Fig. 5*A*, we can estimate that the equilibrium constant L between the two states in a MWC model is approximately 1.0 at 317 K and that the chemical exchange rate is faster than 1,000 s^{-1} (*SI Appendix*, *Text* S4). Whereas the free repressor exists in a dynamic equilibrium, binding of the operator or inducer to their respective binding site shifts this equilibrium to either one or the other of these two states, at the same time

maintaining the symmetry of the dimer. In fact, such conformational equilibrium is also present in the free Lac dimer core (Fig. 3*E*) and found to shift with temperature (*SI Appendix*, Fig. S4), providing further support for the presence of a conformational equilibrium in the free Lac repressor.

Discussion

In this study, major functional states of the Lac repressor could be characterized under comparable conditions using NMR. By monitoring the chemical shift behavior upon inducer binding to either the core dimer domain or to the Lac repressor–operator complex, residues that are critical for inducer signal transfer in the system were identified (*SI Appendix*, *Text* S2). Notably, the same set of residues had been implicated before in genetic studies (44, 45) and following the analysis of crystal structures (24, 27) (*SI Appendix*, Fig. S2). Therefore, the NMR method we used is a sensitive, independent, and reliable tool to identify conformational changes that may occur upon binding of effectors.

With current NMR data, we managed to resolve a persistent discrepancy about the nature of the ligand-free form of the Lac repressor. The free Lac repressor shows to be a highly dynamic molecule, able to adopt a multitude of conformations. This is not only the case for the headpiece, which we show to be positionally disordered vs. the dimeric core and where a flexible hinge region has some alpha-helical propensity, but notably also for the core N-subdomain domain, that—even in the free state—exists in an equilibrium between DNA-bound and inducer-bound conformations. Whereas early T-jump experiments showed already that a rapid conformational transition between two states takes place in the Lac repressor in the absence of any inducers (46), the amplitude of the fast relaxation effect decreased with increasing IPTG concentration, showing the presence of a dynamic equilibrium that can be tuned by the inducer. In line with the classical MWC model, that postulates that in the absence of ligands a protein is in equilibrium between two reversibly accessible states, the linear chemical shift pattern observed for many residues in the N-subdomain of the dimeric Lac repressor demonstrates that binding of either allosteric effector shifts this pre-existing dynamic equilibrium toward one of the extreme states (Fig. 5*B*). This clearly shows that the N-subdomain functions as a regulatory switch, consistent with a MWC model. Both upon binding of DNA and of IPTG the transition is concerted for both protomers of the dimer without significantly populating intermediate states as judged from the absence of extra resonances for intermediate conformations. Also, this conservation of symmetry in the allosteric transitions agrees well with the MWC model.

Recently, a quite different model describing the Lac repressor allostery has been proposed (18). The approach that was used to come to a "dynamic model" relied on a combination of hydrogen–deuterium exchange with mass spectrometry (HDX/MS) and computational modeling of distinct Lac repressor complexes. The conclusion of this study was that the allostery in the bacterial Lac system follows ligand-induced changes in dynamics of the repressor, disagreeing with our findings that are in perfect agreement with a conformational MWC pre-equilibrium. In fact, their arguments are largely based on the crystal structures of the free, inducer-bound, and operator-bound Lac repressor, which are all very similar (less than 1.5 Å difference). However, as we have shown here by NMR spectroscopy, the conformations of the Lac repressor in inducer-bound and operator-bound states in solution differ in fact considerably from each other and the free form can be properly described as a fast-exchange equilibrium of these two states. Apparently this was not detected by X-ray crystallography, potentially due to crystal packing forces.

Even though expression repression and activation steps are relatively well understood, there is still no consensus on how the signal from inducer binding is transferred from the core to the headpiece in the Lac repressor to cause a decrease in DNA binding affinity. Early on, it has been argued that physical pulling of the hinge helix from the minor groove of the operator as a result of the reorientation of the N-subdomains reduces the affinity of the repressor for the operator (24). Later, the observation of persistent interdomain contacts between HP and core in the high-resolution structure of the operator-bound complex (27) together with the results of genetic studies (44) highlighted the importance of these interactions in the allosteric mechanism. This led Bell and Lewis (27) to propose that the release of the hinge helix from the minor groove of the operator may rather be the result of an alteration of intersubunit interactions rather than physical displacement. Unfortunately, up to now X-ray structures of free and IPTG-bound repressor could not resolve this conundrum, since in the absence of DNA both systems lack electron density for the headpiece. However, the NMR analysis of the ternary Lac repressor–operator–inducer complex permits us now to suggest a model for the transition from an operator-bound repressed state to a lower affinity state triggered by inducer binding. We have shown that the observed allosteric effects caused by the inducer in the ternary system involve loss of contacts between the core domain and the headpiece. At this point, at NMR concentrations, the two headpieces in the dimer remain bound to the operator, albeit with only partially structured hinge helices. Before, Taraban et al. (47) characterized a similar ternary complex of Lac repressor–operator–inducer using a different protein construct by small-angle X-ray scattering (SAXS), and also their measurements indicated no complete unfolding of the hinge helix. However, the NMR data additionally show that the stability of the hinge helices is—at least in part—also compromised due to the internal dynamics, and both events result in a reduced affinity of Lac repressor for the operator. Next, in vivo, the large excess of the non-specific low-affinity DNA-binding sites will effectively compete with the *lac* operator DNA causing the Lac repressor to release from the operator. The preferential non-specific DNA binding could then result in further unfolding of the hinge helices (48).

Even though our data agree well with a two-state MWC model, in a large multidomain protein binding multiple ligands, additional structural states may also contribute to its allosteric regulation (3–5). In addition, entropic effects can play an important role in effector affinities and transitions between allosteric states (10, 11, 49, 50). In fact, DNA binding of Lac repressor is clearly associated with the concerted folding of the two hinge helices that reside between the headpieces and the core dimer. These helices are very stable when bound to the operator (48), become dynamic in the ternary complex with operator and inducer, and are largely unfolded in the free Lac repressor. Such changes in flexibility are inevitably associated with entropy changes and certainly contribute to the stabilities of the different allosteric states. In principle, a system with different microstates, even in fast exchange, with concerted IPTG binding, and hinge helices folding could give rise to a large number of uniquely observable and excited states (49–52). Still, even though more complicated models cannot be excluded, our data can be properly brought in agreement with a quite simple MWC-model for activation of gene expression. It is remarkable that only two conformational states of the Lac dimer core play a significant role in the allostery of the Lac repressor.

Recently Changeux summarized the characteristics of a MWC model for allostery (6):

(1) the protein is an oligomer of symmetrically organized subunits,
(2) the oligomers exist in a limited number of conformations in thermal equilibrium without added ligands,
(3) binding of the ligands (DNA or inducer for Lac) would shift the equilibrium by binding the conformation for which they have highest affinity, and
(4) the conformational transitions take place in an all-or-nothing concerted fashion for all subunits and with conservation of symmetry.

This is precisely what we observe for the Lac repressor dimer, for which at least three processes in its allosteric mechanism can be distinguished, namely the homotropic cooperative binding of IPTG, the heterotropic coupling of the operator and IPTG binding and the cooperative folding of the hinge helices. The NMR spectra of the different Lac repressor states reveal clear allosteric effects: the twofold symmetry of the dimers in different states, the existence of two distinct conformations (operator bound and inducer bound), and the maintenance of symmetry of the constituent monomers in allosteric transitions. In the free state, Lac repressor shows a fast equilibrium between the two conformational states, and binding either operator or inducer shifts the equilibrium to one or the other state. This all fits the MWC model.

Materials and Methods

Sample Preparation. Plasmids expressing the K84M mutant Lac repressor dimer lac333K84M (residues 1 to 333) or Lac core dimer lac60-333K84M (residues 60 to 333), both including an N-terminal hexahistidine tag, were created as before (39). The core dimer was expressed in *E. coli* strain Rosetta (DE3) pLysS, the Lac dimer in *E.coli* BL21(DE3). For expression of [^{2}H, ^{13}C, ^{15}N]-labeled proteins, cells were grown in M9 minimal medium containing 2 g/L [^{2}H, ^{13}C]-glucose and 0.5 g/L $^{15}NH_4Cl$ in 99.9% D_2O/0.1% H_2O. Proteins were purified using nickel affinity followed by anion exchange HQ chromatography. The Lac repressor dimer was further purified using a Superdex G75 gel filtration column, all described in detail before (39).

IPTG-free Lac repressor dimer was obtained by growing host cells without induction, whereas expression of [^{2}H, ^{13}C, ^{15}N]-labeled core dimer was induced by 1 mM IPTG. In order to remove any bound IPTG molecules and to back-exchange labile ^{2}H atoms for ^{1}H the protein was diluted to 44 μg/mL with 50 mM KP_i buffer (pH 9) and incubated for 3 h at 60 °C. Protein solutions were finally concentrated by ultrafiltration using a 5 kDa cutoff Centricon (Amicon) and simultaneously buffer was exchanged with an NMR suitable buffer. TROSY spectra of back-exchanged [^{2}H, ^{13}C, ^{15}N]-labeled and [^{2}H, ^{15}N]-labeled core dimer grown in auto-induction media (53, 54) were compared to ensure that both were free of IPTG.

HPLC purified palindromic 22 bp (5′-GAATTGTGAGCGCTCACAATTC-3′) *lac* operator (SymL) (Eurogentec) was dissolved in buffer containing 50 mM KP_i (pH 7.5) and 250 mM KCl and annealed by heating the solution to 95 °C for 5 min and slow-cooling over a period of several hours. The two-stranded operator DNA solution was subsequently dialyzed against water and lyophilized.

DNA Bending Assays. DNA bending assays were performed essentially as described in Spronk et al. (25).

NMR Spectroscopy. The NMR sample used for resonance assignments of the free core dimer contained ~0.6 mM [^{2}H, ^{13}C, ^{15}N]-labeled protein in 50 mM KP_i (pH 6.5), 1 mM dithiothreitol (DTT), 400 mM [*U*-^{2}H]-glycine, 5 % D_2O and 0.01 % NaN_3. The NMR sample to study the protein–DNA complex contained 0.1 mM of [^{2}H, ^{13}C, ^{15}N]-labeled Lac repressor dimer mixed with an equimolar amount of SymL in 20 mM KP_i (pH 6.5), 1 mM DTT, 10 mM KCl, 5 % [*U*-^{2}H]-glycerol, 5% D_2O, 0.01% NaN_3 and a trace amount of EDTA-free protein inhibitor cocktail (Roche). To form the ternary complex, 50 times excess of IPTG was added to the protein–DNA complex. Unfortunately, the limited stability of the Lac repressor dimer in the apo form precluded recording of the spectra that are necessary for its backbone assignment. Instead, the backbone of the HP-less unbound core dimer was assigned and its assignments were subsequently transferred to the Lac repressor dimer. Assignments of the backbone amide protons of the headpiece were available from previous studies (25, 55).

All NMR spectra were acquired on a Bruker AVANCE 900 MHz spectrometer equipped with a TCI HCN cryoprobe. For the backbone assignment of the [^{2}H, ^{13}C, ^{15}N]-labeled Lac repressor core dimer 3D TROSY-HNCA, TROSY-HNCOCA, TROSY-HNCO, TROSY-HNCACO, TROSY-HNCACB (56) and a 3D NOESY-^{15}N-HSQC (57) were recorded at 318 K. The substantial chemical shift differences between apo and IPTG-bound core dimer required de novo resonance assignment also of the IPTG-bound form of the core dimer, whereas assignments of the Lac repressor dimer in complex with operator DNA were confirmed by 3D TROSY-HNCA.

All NMR data were processed using NMRPipe (58) and analyzed with NMRView (59). The combined ^{1}H and ^{15}N chemical shift change (in ppm) of a particular residue upon ligand binding was calculated as $\Delta\delta = [\Delta\delta_{HN}{}^2 + (\Delta\delta_N/R_{scale})^2]^{1/2}$, where the chemical shift scaling factor, $R_{scale} = 6.5$ (60). Data were mapped to existing crystal structures of the Lac repressor using Pymol 0.99 (61).

NMR Relaxation Measurements. For the backbone amides of the DNA-binding domain in the Lac dimer, ^{15}N R_1 and R_2 relaxation rates and ^{15}N-^{1}H-heteronuclear Overhauser enhancements (hetNOE) were determined essentially according to Farrow et al. (62) using a Bruker 600 MHz spectrometer. To obtain R_1 and R_2 a two-parameter exponential was fitted to the experimental intensity decay as a function of the relaxation delay using CurveFit (A. G. Palmer; Columbia University, New York, USA; http://www.palmer.hs.columbia.edu). Relaxation data for the isolated headpiece HP56 used for comparison were taken from ref. 41. Rotational correlation times (τ_c) were obtained from R_2/R_1 ratios and compared to predicted values using the program HYDRONMR assuming rigid body structures (63).

Data, Materials, and Software Availability. All study data are included in the article and/or *SI Appendix*.

ACKNOWLEDGMENTS. Dr. J. Grinstead is acknowledged for critical reading of the manuscript. S. J. de Vries is acknowledged for providing scripts for the analysis of some chemical shift data. R.K. and R.B. were supported by the Netherlands Foundation for Chemical Research (NWO-CW, 175.107.301.10; 700.52.303; and 700.53.103). R.B. was supported by the European Commission (project 031220, Spine2-complexes; project RII3-026145, EU-NMR; project 261863, BioNMR; and project 228461, East-NMR). M.G. was supported by a stipend of the Deutsche Forschungsgemeinschaft (DFG, project 5444273).

Author affiliations: [a]NMR Spectroscopy, Bijvoet Centre for Biomolecular Research, Utrecht University, 3584 CH Utrecht, The Netherlands

1. J. Monod, J. Wyman, J.-P. Changeux, On the nature of allosteric transitions: A plausible model. *J. Mol. Biol.* **12**, 88–118 (1965).
2. D. E. Koshland, G. Nemethy, D. Filmer, Comparison of experimental binding data and theoretical models in proteins containing subunits. *Biochemistry* **5**, 365–385 (1966).
3. R. Phillips, *The Molecular Switch: Signaling and Allostery* (Princeton University Press, 2020.
4. M. Eigen, New looks and outlooks on physical enzymology. *Q. Rev. Biophys.* **1**, 3–33 (1968).
5. V. J. Hilser, J. O. Wrabl, H. N. Motlagh, Structural and energetic basis of allostery. *Annu. Rev. Biophys.* **41**, 585–609 (2012).
6. J.-P. Changeux, The origins of allostery: From personal memories to material for the future. *J. Mol. Biol.* **425**, 1396–1406 (2013).
7. A. P. Kornev, S. S. Taylor, Dynamics-driven allostery in protein kinases. *Trends Biochem. Sci.* **40**, 628–647 (2015).
8. J. Guo, H. X. Zhou, Protein allostery and conformational dynamics. *Chem. Rev.* **116**, 6503–6515 (2016).
9. J. Wyman, D. W. Allen, The problem of the heme interactions in hemoglobin and the Bohr effect. *J. Polymer Sci.* **7**, 499–518 (1951).
10. A. Cooper, D. T. Dryden, Allostery without conformational change. A plausible model. *Eur. Biophys. J.* **11**, 103–109 (1984).
11. R. Nussinov, C.-J. Tsai, Allostery without a conformational change? Revisiting the paradigm. *Curr. Opin. Struct. Biol.* **30**, 17–24 (2015).
12. R. B. O'Gorman *et al.*, Equilibrium binding of inducer to Lac repressor-operator DNA complex. *J. Biol. Chem.* **255**, 10107–10114 (1980).
13. J. P. Changeux, S. Edelstein, Conformational selection or induced fit? 50 years of debate resolved. *F1000 Biol Rep.* **3**, 19 (2011).

14. M. Lewis, The Lac repressor. *C. R. Biol.* **328**, 521–548 (2005).
15. M. Lewis, A tale of two repressors. *J. Mol. Biol.* **409**, 14–27 (2011).
16. R. Daber, K. Sharp, M. Lewis, One is not enough. *J. Mol. Biol.* **392**, 1133–1144 (2009).
17. R. Daber, M. A. Sochor, M. Lewis, Thermodynamic analysis of mutant Lac repressors. *J. Mol. Biol.* **409**, 76–87 (2011).
18. A. Glasgow *et al.*, Ligand-specific changes in conformational flexibility mediate long-range allostery in the Lac repressor. *Nat. Commun.* **14**, 1179 (2023).
19. B. Müller-Hill, *The lac Operon: A Short History of a Genetic Paradigm* (De Gruyter Inc., Berlin/Boston, Germany, 1996).
20. A. Jobe, S. Bourgeois, Lac repressor–operator interaction: VI. The natural inducer of the lac operon. *J. Mol. Biol.* **69**, 397–404 (1972).
21. F. Jacob, J. Monod, On the regulation of gene activity. *Cold Spring Harb. Symp. Quant. Biol.* **69**, 397–404 (1961).
22. C. J. Wilson, H. Zhan, L. Swint-Kruse, K. S. Matthews, The lactose repressor system: Paradigm for regulation, allosteric behavior and protein folding. *Cell. Mol. Life Sci.* **64**, 3–16 (2007).
23. R. Kaptein, E. R. P. Zuiderweg, R. M. Scheek, R. Boelens, W. F. van Gunsteren, A protein structure from nuclear magnetic resonance data: Lac repressor headpiece. *J. Mol. Biol.* **182**, 179–182 (1985).
24. M. Lewis *et al.*, Crystal structure of the lactose operon repressor and its complexes with DNA and inducer. *Science* **271**, 1247–1254 (1996).
25. C. A. E. M. Spronk *et al.*, Hinge-helix formation and DNA bending in various Lac repressor–operator complexes. *EMBO J.* **18**, 6472–6480 (1999).
26. C. A. E. M. Spronk *et al.*, The solution structure of Lac repressor headpiece 62 complexed to a symmetrical *lac* operator. *Structure* **7**, 1483–1492 (1999).
27. C. E. Bell, M. Lewis, A closer view of the conformation of the Lac repressor bound to operator. *Nature Struct. Biol.* **7**, 209–214 (2000).
28. C. G. Kalodimos *et al.*, Plasticity in protein-DNA recognition: Lac repressor interacts with its natural operator *O1* through alternative conformations of its DNA-binding domain. *EMBO J.* **21**, 2866–2876 (2002).
29. A. M. Friedman, T. O. Fischmann, T. A. Steitz, Crystal structure of the Lac repressor core tetramer and its implications for DNA looping. *Science* **268**, 1721–1727 (1995).
30. R. Daber, S. Stayrook, A. Rosenberg, M. Lewis, Structural analysis of Lac repressor bound to allosteric effectors. *J. Mol. Biol.* **370**, 609–619 (2007).
31. A. D. Riggs, R. F. Newby, S. Bourgeois, Lac repressor–operator interaction: II. Effect of galactosides and other ligands. *J. Mol. Biol.* **51**, 303–314 (1970).
32. S. L. Laiken, C. A. Gross, P. H. von Hippel, Equilibrium and kinetic studies of *Escherichia coli* Lac repressor-inducer interactions. *J. Mol. Biol.* **66**, 143–155 (1972).
33. R. B. O'Gorman, K. S. Matthews, Fluorescence and ultraviolet spectral studies of Lac repressor modified with N-bromosuccinimide. *J. Biol. Chem.* **252**, 3572–3577 (1977).
34. P. A. Whitson, A. A. Burgum, K. S. Matthews, Trinitrobenzenesulfonate modification of the lysine residues in lactose repressor protein. *Biochemistry* **23**, 6046–6052 (1984).
35. T. J. Daly, K. S. Matthews, Allosteric regulation of inducer and operator binding to the lactose repressor. *Biochemistry* **25**, 5479–5484 (1986).
36. K. Pervushin, R. Riek, G. Wider, K. Wüthrich, Attenuated T_2 relaxation by mutual cancellation of dipole–dipole coupling and chemical shift anisotropy indicates an avenue to NMR structures of very large biological macromolecules in solution. *Proc. Natl. Acad. Sci. U.S.A.* **94**, 12366–12371 (1997).
37. J. Fiaux, E. B. Bertelsen, A. L. Horwich, K. Wüthrich, NMR analysis of a 900K GroEL-GroES complex. *Nature* **418**, 207–211 (2002).
38. V. Tugarinov, W.-Y. Choy, V. Y. Orekhov, L. E. Kay, Solution NMR-derived global fold of a monomeric 82-kDa enzyme. *Proc. Natl. Acad. Sci. U.S.A.* **102**, 622–627 (2005).
39. J. Romanuka, H. V. D. Bulke, R. Kaptein, R. Boelens, G. E. Folkers, Novel strategies to overcome expression problems encountered with toxic proteins: Application to the production of Lac repressor proteins for NMR studies. *Protein Expr. Purif.* **67**, 104–112 (2009).
40. L. P. Gerk, O. Leven, B. Müller-Hill, Strengthening the dimerisation interface of Lac repressor increases its thermostability by 40 °C. *J. Mol. Biol.* **299**, 805–812 (2000).
41. M. Slijper *et al.*, Backbone and side chain dynamics of Lac repressor headpiece (1–56) and its complex with DNA. *Biochemistry* **36**, 249–254 (1997).
42. N. Geisler, K. Weber, Isolation of the amino-terminal fragment of lactose repressor necessary for DNA binding. *Biochemistry* **16**, 938–943 (1977).
43. M. D. Barkley, A. D. Riggs, A. Jobe, S. Bourgeois, Interaction of effecting ligands with Lac repressor and repressor–operator complex. *Biochemistry* **14**, 1700–1712 (1975).
44. J. Suckowa *et al.*, Genetic studies of the Lac repressor XV: 4000 single amino acid substitutions and analysis of the resulting phenotypes on the basis of the protein structure. *J. Mol. Biol.* **261**, 509–523 (1996).
45. H. C. Pace *et al.*, Lac repressor genetic map in real space. *Trends Biochem. Sci.* **22**, 334–339 (1997).
46. F. Y. H. Wu, P. Bandyopadhyay, C.-W. Wu, Conformational transitions of the Lac repressor from *Escherichia coli*. *J. Mol. Biol.* **100**, 459–472 (1976).
47. M. Taraban *et al.*, Ligand-induced conformational changes and conformational dynamics in the solution structure of the lactose repressor protein. *J. Mol. Biol.* **376**, 466–481 (2008).
48. C. G. Kalodimos *et al.*, Structure and flexibility adaptation in nonspecific and specific protein-DNA complexes. *Science* **305**, 386–389 (2004).
49. N. Popovych, S. Sun, R. H. Ebright, C. G. Kalodimos, Dynamically driven protein allostery. *Nat. Struct. Mol. Biol.* **13**, 831–838 (2006).
50. S.-R. Tzeng, C. G. Kalodimos, Protein dynamics and allostery: An NMR view. *Curr. Opin. Struct. Biol.* **21**, 62–67 (2011).
51. F. A. A. Mulder, A. Mittermaier, B. Hon, F. W. Dahlquist, L. E. Kay, Studying excited states of proteins by NMR spectroscopy. *Nat. Struct. Biol.* **8**, 932–935 (2001).
52. A. J. Baldwin, L. E. Kay, NMR spectroscopy brings invisible protein states into focus. *Nat. Chem. Biol.* **5**, 808–814 (2009).
53. F. W. Studier, Protein production by auto-induction in high-density shaking cultures. *Protein Expr. Purif.* **41**, 207–234 (2005).
54. R. C. Tyler *et al.*, Auto-induction medium for the production of [*U*-^{15}N]- and [*U*-^{13}C, *U*-^{15}N]-labeled protein for NMR screening and structure determination. *Protein Expr. Purif.* **40**, 268–278 (2005).
55. M. Slijper, A. M. J. J. Bonvin, R. Boelens, R. Kaptein, Refined structure of Lac repressor headpiece (1–56) determined by relaxation matrix calculations from 2D and 3D NOE data: Change of tertiary structure upon binding to the *lac* operator. *J. Mol. Biol.* **259**, 761–773 (1996).
56. M. Salzmann, K. Pervushin, G. Wider, H. Senn, K. Wüthrich, TROSY in triple-resonance experiments: New perspectives for sequential NMR assignment of large proteins. *Proc. Natl. Acad. Sci. U.S.A.* **95**, 13585–13590 (1998).
57. J. Cavanagh, W. J. Fairbrother, A. G. Palmer, M. Rance, N. J. Skelton, *Protein NMR Spectroscopy: Principles and Practice* (Elsevier Academic Press, 2007).
58. F. Delaglio *et al.*, NMRPipe: A multidimentional spectral processing system based on UNIX pipes. *J. Biomol. NMR* **6**, 277–293 (1995).
59. B. A. Johnson, R. A. Blevins, NMRView: A computer program for the visualization and analysis of NMR data. *J. Biomol. NMR* **4**, 603–614 (1994).
60. F. A. A. Mulder, D. Schipper, R. Bott, R. Boelens, Altered flexibility in the substrate-binding site of related native and engineered high-alkaline Bacillus subtilisins. *J. Mol. Biol.* **292**, 111–123 (1999).
61. W. L. DeLano, The PyMOL molecular graphics system (Version 0.99, DeLano Scientific LLC, San Carlos, CA, USA, 2002).
62. N. A. Farrow *et al.*, Backbone dynamics of a free and a phosphopeptide-complexed Src homology 2 domain studied by ^{15}N NMR relaxation. *Biochemistry* **33**, 5984–6003 (1994).
63. J. G. de la Torre, M. L. Huertas, B. Carrasco, HYDRONMR: Prediction of NMR relaxation of globular proteins from their atomic-level structure. *J. Magn. Reson.* **147**, 138–146 (2000).